TOWARDS A MATERIAL POINT METHOD VOCAL TRACT SIMULATION

Scott R. Moisik

Nanyang Technological University
scott.moisik@ntu.edu.sg

ABSTRACT

The material point method (MPM) is a powerful numerical approach to the simulation of deformable bodies. It benefits from not requiring an explicit computational mesh to discretize a body, and this allows for myriad simulation possibilities including large deformations, fracture, phase change, mixture, and interactions between different materials, even with different phases (e.g., solid-fluid interaction). This paper reports the preliminary work on applying the MPM with the goal of creating a comprehensive 3D simulation environment for studying vocal tract biomechanics, aerodynamics, and acoustics (and the interaction of these).

Keywords: 3D vocal tract simulation, material point method

1. INTRODUCTION

The vocal tract is a complex collection of biological tissues. The main approach to three-dimensional computational simulation of vocal tract structures has been via the finite element method (FEM; e.g., [1]–[4]). A FEM simulation is principally defined by a collection of computational meshes, which provide a spatial discretization of any deformable bodies being simulated. Bodies that are very stiff, like bony structures, can be treated as rigid bodies (possessing only six rigid degrees of freedom, three translational and three rotational modes, and thus lacking deformation modes). This is an approximation given that even very stiff structures of the vocal tract can still undergo small deformation, but the loads experienced during speech production are small enough that these deformations can be entirely neglected. While the FEM approach benefits from possessing excellent accuracy in numerically solving the equations of motion over complex domains and from being relatively light-weight in computational burden, the strong dependency on computational meshes presents serious challenges. In particular, vocal tract structures like the tongue can undergo large deformations that excessively distort elements, reducing accuracy and stability (see [5]). Developing meshes with good computational properties is not a trivial matter and automated algorithms do not always produce useful results. Thus, there is a desire for numerical techniques that do away with the strong dependence on a computational mesh, such as the material point method (MPM).

1.1. Material point method (MPM): Background

The MPM was originally proposed by Sulsky et al. [6] as an extension of the particle-in-cell method, a well-known technique for fluid dynamics simulation [7], to the simulation of solid bodies. The MPM shares conceptual DNA with other fluid dynamics methods, such as smoothed-particle hydrodynamics [8]. It uses stateful particles (or packets/volumes) of mass to discretize a material of interest (be it a simple fluid like water or even more exotic matter like plasma or an entire star) and integration of key properties represented by the distribution of such particles is performed via kernel or shape functions.

One of the benefits of the MPM is that, because materials transfer their momentum to a shared background grid, it is possible to effortlessly simulate contacts and collisions between deformable bodies. There is no need for explicit contact detection and collision response handling, as communication between disjoint bodies (and even different parts of the same body in self-collision), occurs when the momenta of material points from interacting bodies are accumulated on the background grid. The down-side to this is that the resolution of the background grid dictates the resolution of the contact interface, with coarser grids leaving a small separation between bodies coming into contact. Another major challenge with shared background grids is that interaction between materials is sticky: that is, the ordinary formulation of the MPM imposes an obligatory no-slip boundary condition on interacting bodies. The practical consequence of this is that separate materials cannot simply slide past each other, but rather experience infinite friction and thus exhibit a sticking behaviour when coming into close contact.

2. MPM VOCAL TRACT SIMULATION

In this work, the development of a simulation environment is described that is intended for simulation of vocal tract structure biomechanics and interaction with aerodynamic and acoustic flows. Currently, the MPM is the sole approach used (although it is possible to mix the MPM with other

numerical approaches, including finite elements, as in [9]). Progress towards the goal of a comprehensive general-purpose solution for vocal tract simulation is underway but certainly not finished, and the focus here is to report on steps taken towards the biomechanical component while also describing some proof-of-concept examples that use the MPM for simulating vocal tract aerodynamics and acoustics.

2.2. Simulation of rigid bodies

While the MPM is a strong choice for simulating deformable solids and fluids, like in FEM simulation, stiff bodies can pose numerical stability issues if the appropriate integration scheme is not used. This means that a strategy is required to effectively handle rigid bodies, like the mandible and hyoid bone.

Rigid bodies can be modelled separately via traditional methods for simulating rigid body mechanics (e.g., as might be used in robotics), and this method has been used successfully with the MPM (see, e.g., [10]). Another possibility is to apply a shape correction to a deformable body that limits the body to purely rigid modes of displacement. While the literature contains no record of such an approach being used in the context of the MPM, it has been pursued for another particle-based method known as position based dynamics (PBD) [11]. After a body is updated, its material points are projected to the positions of the same body if it were to only undergo purely rigid transformation. These projected positions are established via Procrustes registration and once the projections are made, a velocity correction is applied to conserve momentum.

2.3. Simulation of muscle contraction

The approach to muscle simulation used here follows the work of Blemker and colleagues (see, e.g., [12]–[14]). These researchers developed a numerical model that approaches muscle tissue as a fiber-reinforced composite embedded within finite-element volumes representing muscle bellies. There is no research on muscle simulation using the MPM, but the concept of fiber-reinforced materials has been explored in [15] with the aim to simulate anisotropic material damage. The implementation here modifies the constitutive law for chains of particles forming muscle fibers to employ the muscle model described by Blemker.

3. DEMONSTRATIONS

To illustrate the capabilities of the vocal tract simulation environment under development, several different demonstrations are presented below that feature different aspects of what is possible with the MPM approach.

3.1. Deformable body simulation

In Fig. 1, Jell-O-like blocks demonstrate the utility of the shared-background grid in automatically handling contact and collision. As the red (top) block shows in its separating bounce in the final (rightmost) frame, despite "sticky" interaction inherent to basic MPM, the objects can still separate if their material properties, constitutive model, and momenta favour pulling local parts of material away in regions of proximity.

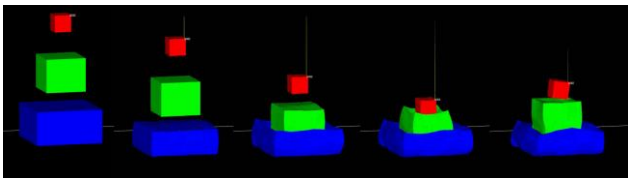

Figure 1: Falling Jell-O-like blocks. A sequence of frames showing the evolution of a simulation where three deformable blocks are dropped and collide into each other demonstrating automatic collision handling on a shared background grid.

3.2. The larynx-hyoid-jaw-tongue model

Currently the lower hull of the vocal tract (Fig. 2), complete with a detailed representation of the larynx (Fig. 3), has been developed. The near term goal is to expand this set of structures to include the lips, maxilla, soft palate, and pharynx. Drawing inspiration from [2], an even more comprehensive set that includes the trachea and cervical spine can also be envisioned.

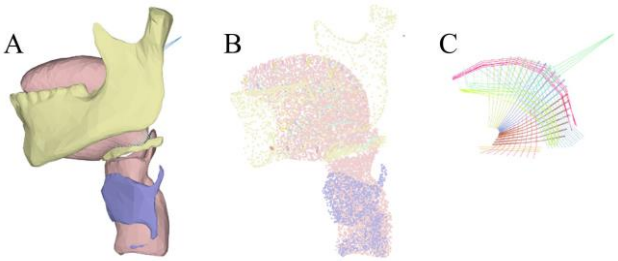

Figure 2: "Lower hull" vocal tract model featuring jaw-tongue-hyoid-larynx complex with laryngeal mucosa. The interior of surface meshes (A) are sampled to identify material points (B). Bodies like the tongue with its lingual muscles (C) are treated as fiber-reinforced composites.

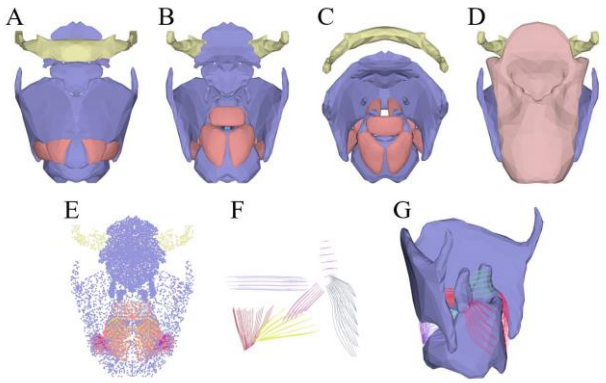

Figure 3: Various views of the larynx model. Surface meshes include the laryngeal cartilages, major internal muscles, and mucosa (A-D). The interior meshes are sampled to generate material points (E), and muscle portions are reinforced by muscle fibers (F-G).

3.2.1. Coupled rigid and deformable bodies

In Fig. 4, the coupling between the tongue and the jaw and the tongue and larynx (via the hyoid bone) is accomplished using invisible springs that simulate the various tendinous and ligamentous connections. More detailed simulation of these structures with material points is also possible. Rigidity of structures like the jaw is enforced using the projection method inspired by PBD described above in Section 2.2.

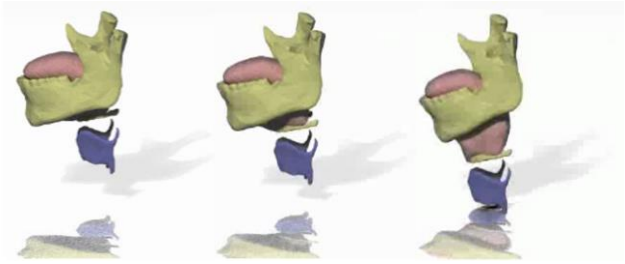

Figure 4: Coupled rigid and deformable bodies simulated under the influence of gravity: (from left-to-right) the larynx-hyoid-jaw-tongue complex starts at rest with the jaw pinned at its condyles and then falls to a resting state when the thyroid collides with the floor.

3.2.2. Muscle simulation

Fig. 5 and Fig. 6 illustrate simulation of tongue and laryngeal muscle action, both using an implementation of the Blemker-style fiber-reinforced muscle model [13]. The sticky (high-friction) interaction between tongue and jaw limits some of the tongue's mobility. Tendons can be implemented using extensibility constraints described in [15] to correct some issues, such as the excessive posterior displacement of the tongue volume in the region of the mental spines in response to genioglossus posterior activity.

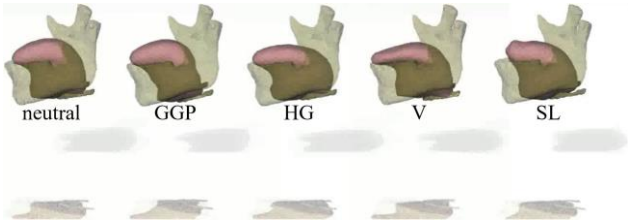

Figure 5: Tongue muscle action: neutral = no muscles active; GGP = genioglossus posterior; HG = hyoglossus; V = vertical; SL = superior longitudinal.

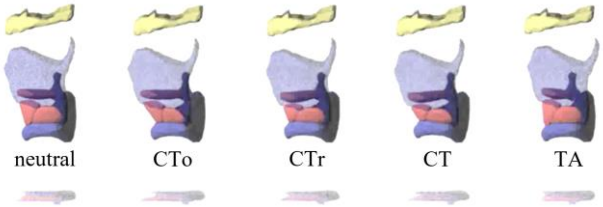

Figure 6: Larynx muscle action: neutral = no muscles active; CTo = cricothyroid pars oblique; CTr = cricothyroid pars recta; CT = cricothyroid (full muscle); TA = (internal) thyroarytenoid.

3.4. Explorations of vocal tract aerodynamics

With the right constitutive model, it is possible to simulate almost any material, including air (see, e.g., [16]). Preliminary tests on aerodynamic and acoustic simulations show promise for simulating phenomena such as ejectives (Fig. 7) and air filled membranes (Fig. 8); with the latter, one possible application is for simulation of the laryngeal air sac of the gibbon.

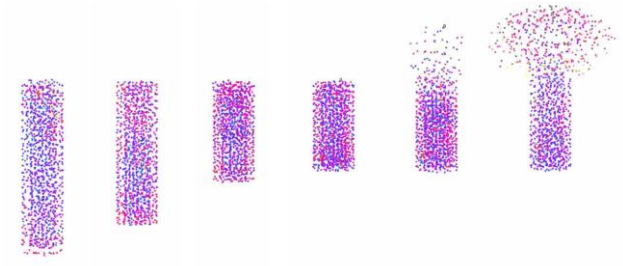

Figure 7: Proof-of-concept ejective simulation. The sequence shows (from left to right) an initially closed vocal tract tube being vertically squashed to emulate (much exaggerated) larynx raising followed by release of the 'oral' stricture at the other end of the tube.

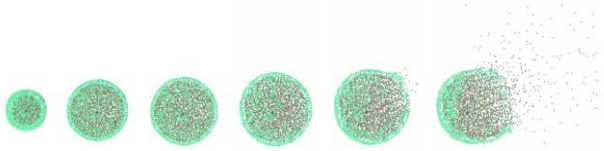

Figure 8: Balloon pop. The sequence shows (from left to right) a membrane filled with compressed air rapidly expanding and then bursting.

3.5. Explorations of vocal tract acoustics

Beyond aerodynamic simulations, the MPM may hold promise for detailed simulation of acoustic and even aeroacoustic phenomena. A proof-of-concept test was made using a constraint surface in the form of the vocal tract in [i] configuration (Fig. 9). The air was subjected to a periodic velocity field near the glottis to simulate the glottal volume velocity. Velocity waves can be seen to bounce around the vocal tract, suggesting transmission of acoustic energy.

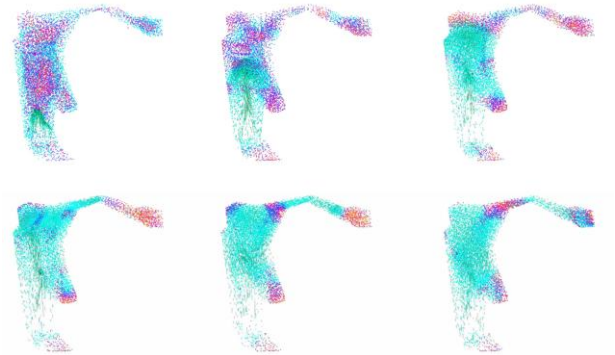

Figure 9: Proof-of-concept [i] acoustics. A 3D vocal tract constraint is filled with air subjected to a glottal volume velocity field. The transmission of wave energy can be seen as the system evolves over time (left to right, top to bottom). Material points are coloured by their speed.

3.6. Fluid-solid interaction: An unconstricted epiglottal trill

The ability to simulate fluid-solid interaction using air within the vocal tract would allow for simulation of a wide range of speech-relevant phenomena involving vibration. As a demonstration, an 'unconstricted' epiglottal trill was simulated using air and the laryngeal mucosa (Fig. 10). Epiglottal trills normally feature strong constriction of the epilarynx, but this proof-of-concept model only uses the mucosa in its neutral state without the laryngeal muscle activity required for constriction. It was necessary to employ separate grids with an explicit collision model to avoid the "sticky" interaction problem.

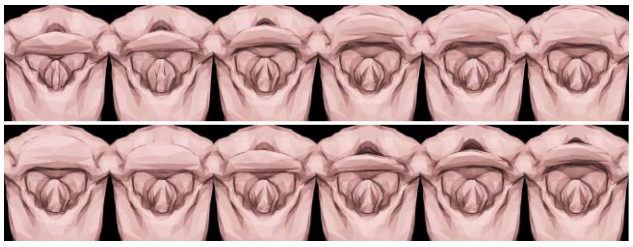

Figure 10: "Unconstricted" epiglottal trill. A sequence of frames (from left to right, top to bottom) showing the laryngeal mucosa interacting with air (not visualized) resulting in vibration of the epiglottis.

4. LIMITATIONS AND FUTURE DIRECTIONS

While the initial explorations of various types of vocal tract simulation are promising, a number of limitations need to be overcome before the model can be used to explore real problems in vocal tract behaviour during speech production (and related areas like singing, swallowing, and so forth). Most important is that the approach to fluid-solid interaction currently employed uses dual and independent background grids to separately update the solid and fluid (air) materials with a collision model to allow for information to flow between the materials. This is not ideal because it undercuts the ability of the MPM to allow for this communication to happen implicitly without any external contact and collision handling. One approach to solving this problem has been proposed by Fang et al. [17] called interface quadrature MPM (IQ-MPM), which employs an air-like "ghost matrix" (analogous to a biological matrix that surrounds and supports living cells). This allows for strong two-way interaction between materials that crucially enables slip boundary conditions, avoiding the sticky-contact problem inherent to 'vanilla' MPM. Another key difficulty is the simulation of very stiff materials. Currently the model only employs explicit integration using the forward Euler numerical scheme to update the equations of motion. The use of an implicit integrator that employs a backward Euler scheme can be implemented to allow for much larger time steps and with much improved numerical stability [18].

5. REFERENCES

[1] F. Alipour, D. A. Berry, and I. R. Titze, "A finite-element model of vocal-fold vibration," *J. Acoust. Soc. Am.*, vol. 108, no. 6, pp. 3003–3012, Nov. 2000, doi: 10.1121/1.1324678.

[2] P. Anderson *et al.*, "Chapter 20 - FRANK: A Hybrid 3D Biomechanical Model of the Head and Neck," in *Biomechanics of Living Organs*, Y. Payan and J. Ohayon, Eds. Oxford: Academic Press, 2017, pp. 413–447. doi: 10.1016/B978-0-12-804009-6.00020-1.

[3] S. Deguchi, Y. Kawahara, and S. Takahashi, "Cooperative regulation of vocal fold morphology and stress by the cricothyroid and thyroarytenoid muscles," *J. Voice*, vol. 25, no. 6, pp. e255–e263, Nov. 2011.

[4] J. E. Lloyd, I. Stavness, and S. S. Fels, "ArtiSynth: A fast interactive biomechanical modeling toolkit combining multibody and finite element simulation," in *Soft tissue biomechanical modeling for computer assisted surgery*, Y. Payan, Ed. Berlin, Germany: Springer, 2012, pp. 355–394.

[5] S. Garg and M. Pant, "Meshfree Methods: A Comprehensive Review of Applications," *Int. J.*

Comput. Methods, vol. 15, no. 04, p. 1830001, Jun. 2018, doi: 10.1142/S0219876218300015.

[6] D. Sulsky, S.-J. Zhou, and H. L. Schreyer, "Application of a particle-in-cell method to solid mechanics," *Comput. Phys. Commun.*, vol. 87, no. 1, pp. 236–252, May 1995, doi: 10.1016/0010-4655(94)00170-7.

[7] F. H. Harlow, "The particle-in-cell method for numerical solution of problems in fluid dynamics," Los Alamos Scientific Lab., N. Mex., LADC-5288, Mar. 1962. doi: https://doi.org/10.2172/4769185.

[8] R. A. Gingold and J. J. Monaghan, "Smoothed particle hydrodynamics: theory and application to non-spherical stars," *Mon. Not. R. Astron. Soc.*, vol. 181, no. 3, pp. 375–389, Dec. 1977, doi: 10.1093/mnras/181.3.375.

[9] C. Jiang, C. Schroeder, A. Selle, J. Teran, and A. Stomakhin, "The affine particle-in-cell method," *ACM Trans. Graph.*, vol. 34, no. 4, pp. 1–10, Jul. 2015, doi: 10.1145/2766996.

[10] Y. Hu *et al.*, "A moving least squares material point method with displacement discontinuity and two-way rigid body coupling," *ACM Trans. Graph.*, vol. 37, no. 4, pp. 1–14, Aug. 2018, doi: 10.1145/3197517.3201293.

[11] M. Müller, B. Heidelberger, M. Teschner, and M. Gross, "Meshless deformations based on shape matching," *ACM Trans. Graph.*, vol. 24, no. 3, pp. 471–478, Jul. 2005, doi: 10.1145/1073204.1073216.

[12] S. S. Blemker and S. L. Delp, "Three-Dimensional Representation of Complex Muscle Architectures and Geometries," *Ann. Biomed. Eng.*, vol. 33, no. 5, pp. 661–673, May 2005, doi: 10.1007/s10439-005-1433-7.

[13] S. S. Blemker, P. M. Pinsky, and S. L. Delp, "A 3D model of muscle reveals the causes of nonuniform strains in the biceps brachii," *J. Biomech.*, vol. 38, no. 4, pp. 657–665, Apr. 2005, doi: 10.1016/j.jbiomech.2004.04.009.

[14] M. Stone *et al.*, "Structure and variability in human tongue muscle anatomy," *Comput. Methods Biomech. Biomed. Eng. Imaging Vis.*, vol. 6, no. 5, pp. 499–507, Sep. 2018, doi: 10.1080/21681163.2016.1162752.

[15] J. Wolper *et al.*, "AnisoMPM: animating anisotropic damage mechanics," *ACM Trans. Graph.*, vol. 39, no. 4, Jul. 2020, doi: 10.1145/3386569.3392428.

[16] W. Hu and Z. Chen, "Model-based simulation of the synergistic effects of blast and fragmentation on a concrete wall using the MPM," *Int. J. Impact Eng.*, vol. 32, no. 12, pp. 2066–2096, Dec. 2006, doi: 10.1016/j.ijimpeng.2005.05.004.

[17] Y. Fang *et al.*, "IQ-MPM: an interface quadrature material point method for non-sticky strongly two-way coupled nonlinear solids and fluids," *ACM Trans. Graph.*, vol. 39, no. 4, Jul. 2020, doi: 10.1145/3386569.3392438.

[18] T. F. Gast, C. Schroeder, A. Stomakhin, C. Jiang, and J. M. Teran, "Optimization Integrator for Large Time Steps," *IEEE Trans. Vis. Comput. Graph.*, vol. 21, no. 10, pp. 1103–1115, Oct. 2015, doi: 10.1109/TVCG.2015.2459687.